

HADRON PRODUCTION IN NEUTRINO INTERACTIONS WITH NUCLEONS AND NUCLEI AT HIGH ENERGIES

Gennady Lykasov

*Joint Institute for Nuclear Research, Dubna,
141980, Moscow region, Russia*

OUTLOOK

I. Motivation to study of $\nu - N$ and $\nu - A$ reactions at high energies

II. $1/N$ expansion in QCD and inclusive $\nu - N$ processes

III. Non perturbative effects at moderate and low Q^2 in $\nu + p \rightarrow \mu^- + X$ reactions

IV. Inclusive and semi-inclusive $\nu + A \rightarrow \mu^- + X$ processes

V. Comparison obtained results with NOMAD data and other calculations

VI. A possible application of suggested approach to analyze the OPERA experiment

VII. Summary

Planar and cylinder graphs

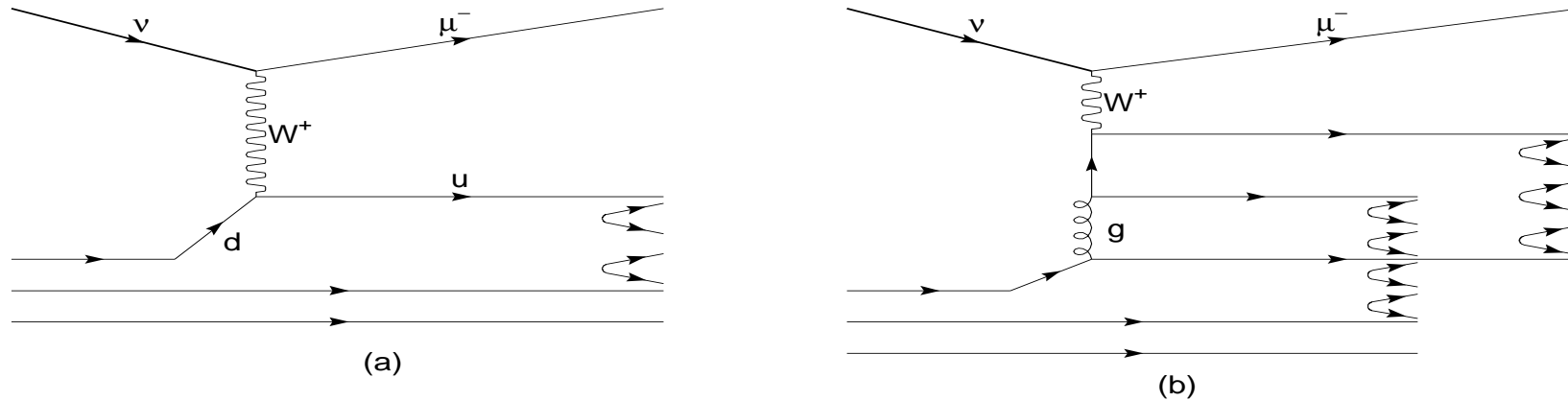


Figure 1: The planar graph (left panel) and the cylinder graph (right panel). *G.Veneziano, Phys.Lett., B52,220 (1974)*

Semi-inclusive process $\nu(\bar{\nu})p \rightarrow \mu^-(\mu^+)hX$

$$\rho_{nu(\bar{\nu})p \rightarrow \mu^-(\mu^+)hX} = E_h \frac{dN}{d^3p_h d\Omega dE'}$$

Relativistic invariant semi-inclusive spectrum

$$\rho_{\nu(\bar{\nu})p \rightarrow \mu^-(\mu^+)hX} = \Phi(Q^2) \{ F_P(x, Q^2; z, p_t) + F_C(x, Q^2; z, p_t) \}$$

with

$$\Phi(Q^2) = mE \frac{G^2}{\pi} \frac{m_W^2}{Q^2 + m_W^2},$$

where G is the Fermi weak coupling constant, E is the energy of incoming neutrino, m and m_W are the nucleon and the W -boson masses respectively. $x = Q^2/2(p_\nu \cdot k)$ is the Bjorken variable, p_ν and k are the four-momenta of the initial neutrino and nucleon, $z = (E_h + p_{hz})/(E + p_z)$ is the light cone variable.

The variable z can be treated also as the Feynman variable $x_F = \frac{2p_L^*}{W_X}$ defined as the longitudinal momentum fraction in the hadronic center mass system (h.c.m.s.), p_L^* is the longitudinal hadron momentum in the h.c.m.s. (*G.L., U.Sukhatme, V.V.Uzhinsky, Phys.Lett.* **B553**,217 (2003))

Mean multiplicity of charged hadron in the current fragmentation region

The multiplicity $\langle n_{ch} \rangle$ measured by NOMAD is close to $\langle n_{ch} \rangle / 2$ results from e^+e^- experiment at $E = \sqrt{s}$ and $\langle n_{ch} \rangle$ from ep and $\bar{\nu}p$ at $E = Q$. **QCD fit for $\langle n_{ch} \rangle$**

$$\langle n_{ch}^{QCD} \rangle = a + b \exp(c \sqrt{\ln(Q^2/Q_0^2)}) ,$$

where $a=2.257$, $b=0.094$, $c=1.775$, $Q_0=1\text{GeV.c.}$ (*W.Furmanski, R.Petronzio, S.Pokorski, Nucl.Phys.***B155**,253 (1979); *A.Bassetto, M.Ciafaloni, G.Marchesini, Phys.Lett.***B83**, 207(1979); *K.Konishi, Rutherford Report RL 79-035 (1979); A.H.Mueller, Phys.Lett.***B213**, 85(1983))

Multiple hadron production in $\nu - p \rightarrow \mu^- + X$ process

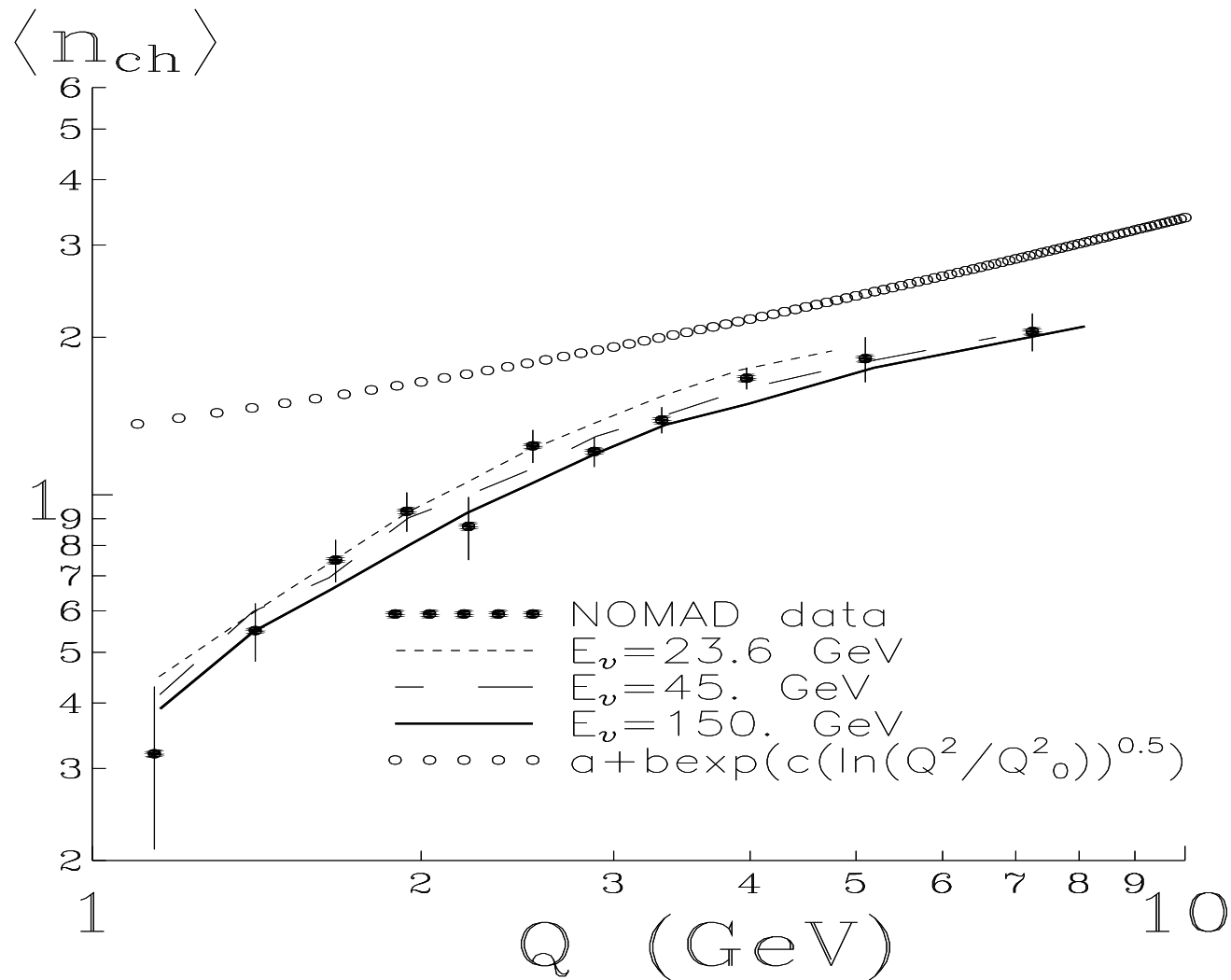


Figure 2: Mean multiplicity of charged hadron in the current fragmentation region as a function of the momentum transfer Q . The open circles correspond to the QCD fit; the solid, long dash and short dash lines correspond to our calculations at $E_\nu = 150$.GeV, 45.GeV and $E_\nu = 23.6$.GeV respectively. The experimental points are the NOMAD data.

Q^2 -inclusive spectrum

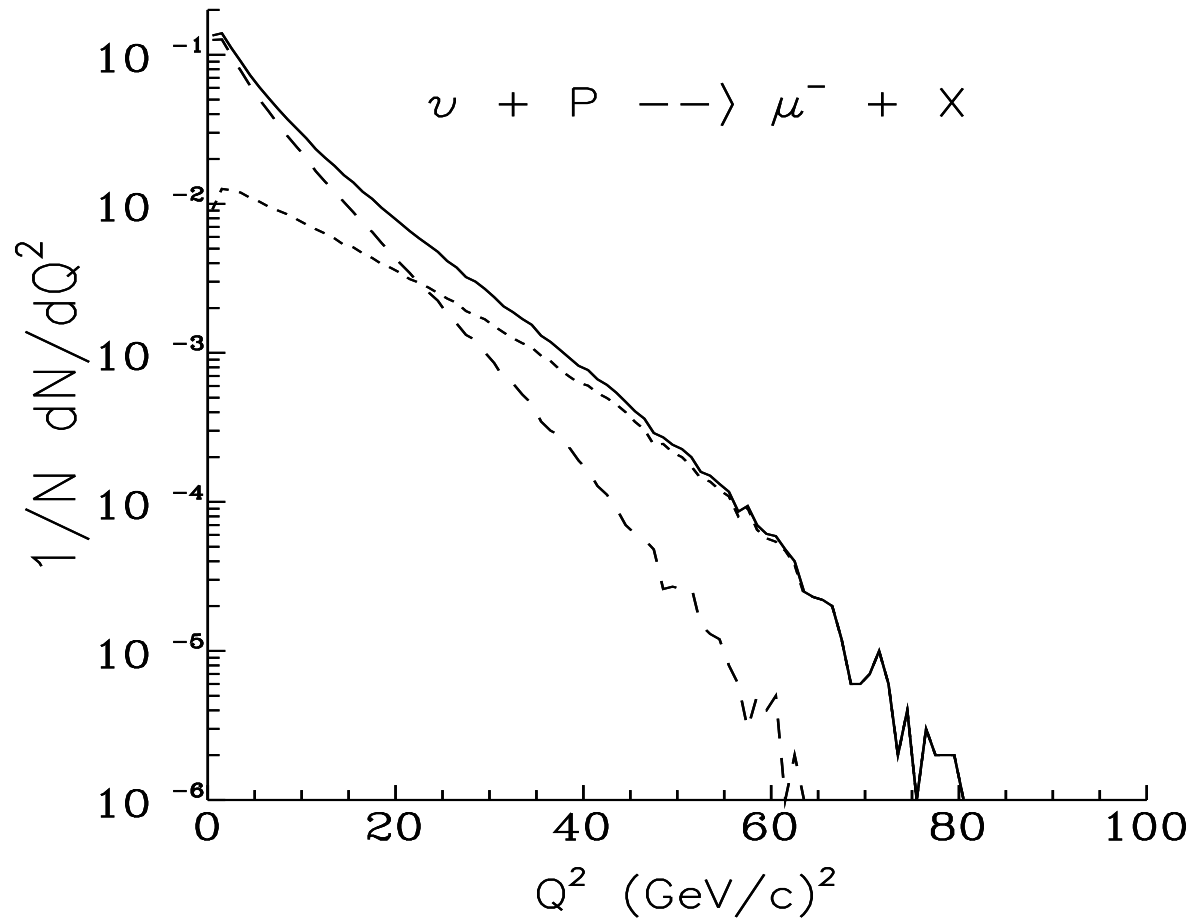


Figure 3: The Q^2 -distribution $\frac{1}{N} \frac{dN}{dQ^2}$ of muons produced in $\nu p \rightarrow \mu^- X$ reaction. The long dash and short dash lines correspond to the contributions of the cylinder and planar graphs respectively. The solid line is the sum of these contributions.

x_F -distributions of strange hadron

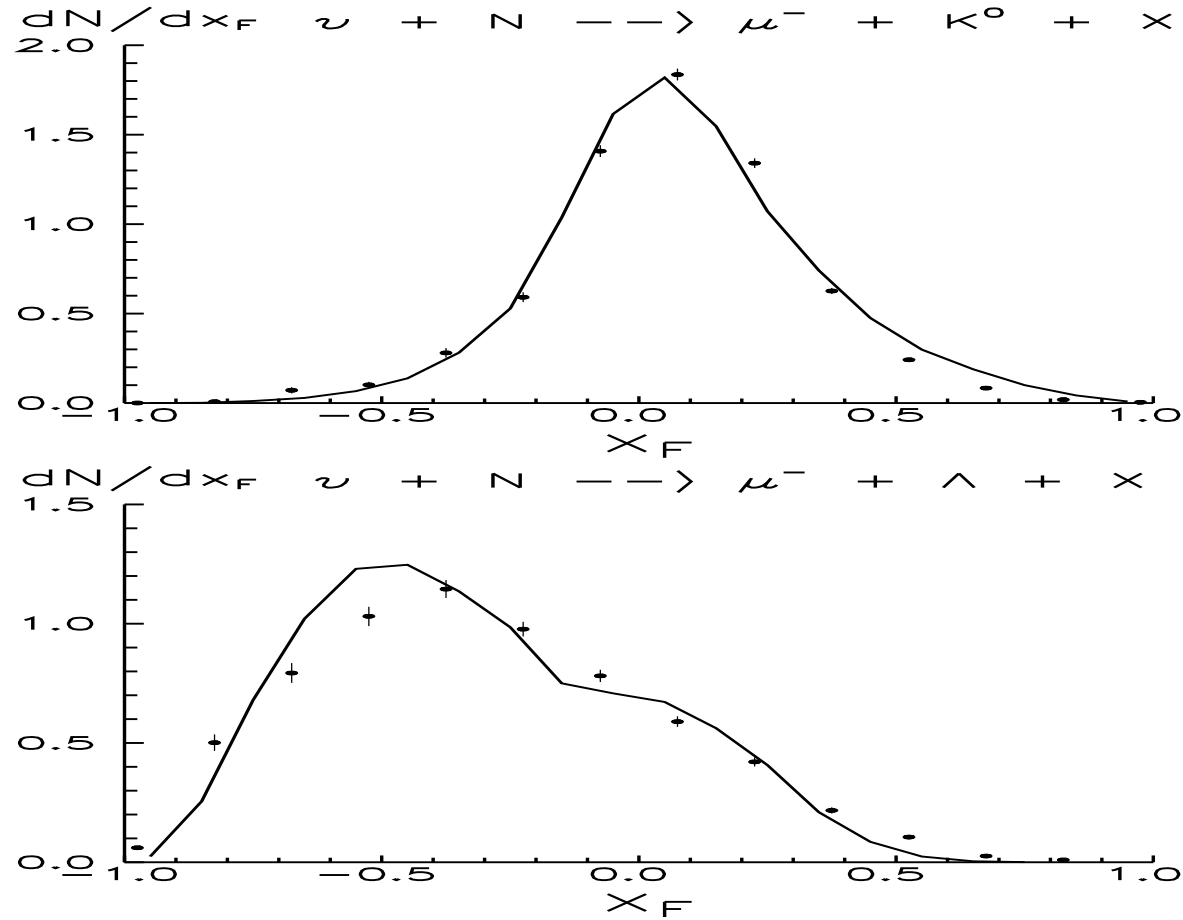


Figure 4: The x_f -distribution of strange hadron dN/dx_F . produced in $\nu p \rightarrow \mu^- X$ reaction.

Multiplicity of strange hadrons

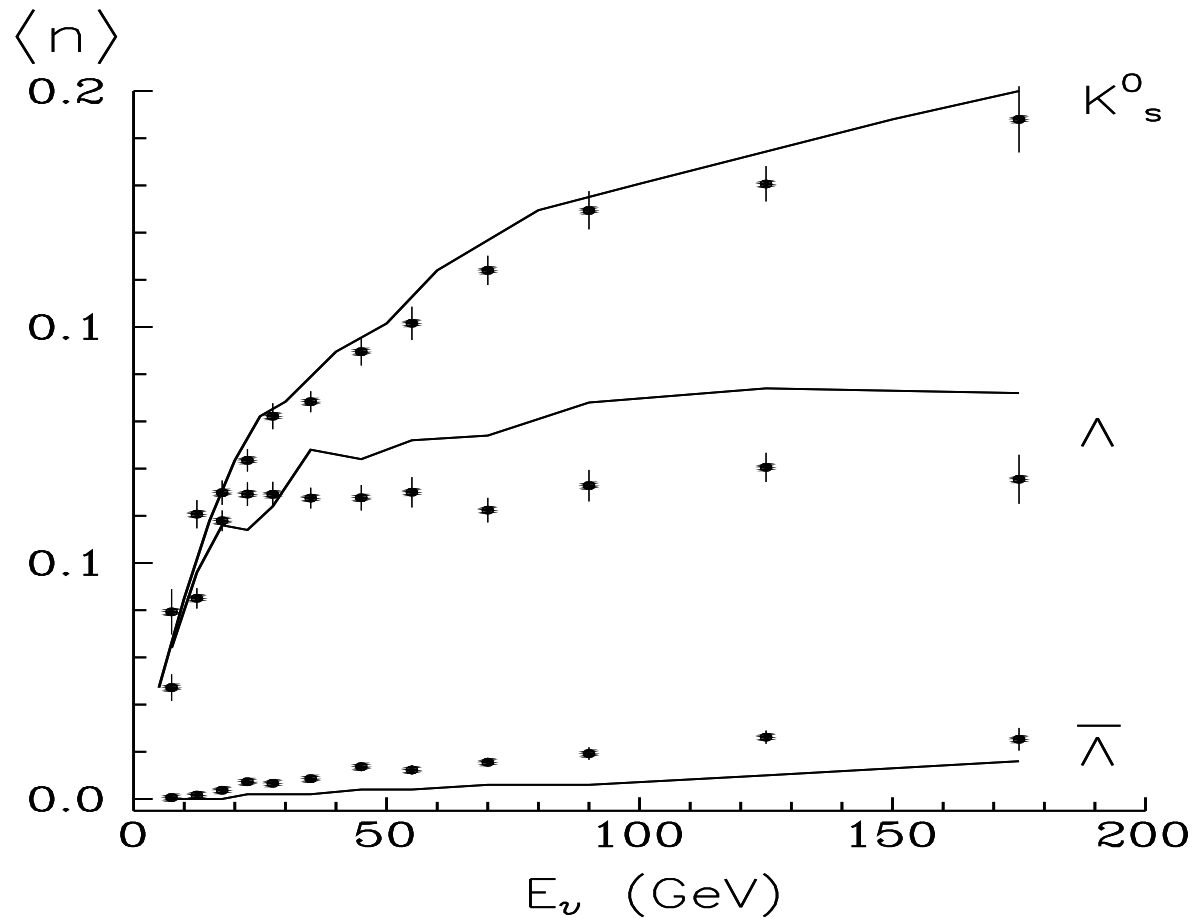


Figure 5: The multiplicity of strange hadron as a function of neutrino energy E_ν .

MC calculation of K_S^0 -spectra

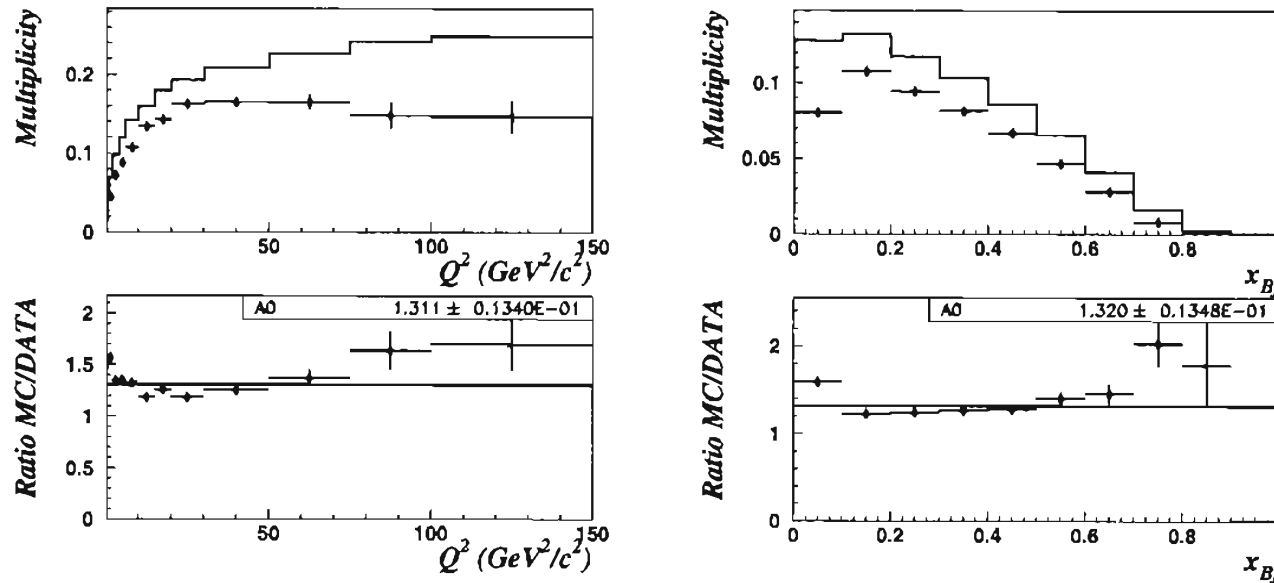


Fig. 6. Yields in the default MC (histogram) and in the data (points with error bars) for K_S^0 as a function of E_ν , W^2 , Q^2 and x_{Bj} . The MC/Data ratios and their fit to a constant are also shown.

Figure 6: The multiplicity of K_S^0 and ratio MC/DATA as a function of Q^2 and x_B , MC(histogram) calculation and the NOMAD data (points with errorbars).

(P.Astier (NOMAD Coll.), Nucl.Phys.**B621**, (2002))

MC calculation of K_S^0 -spectra

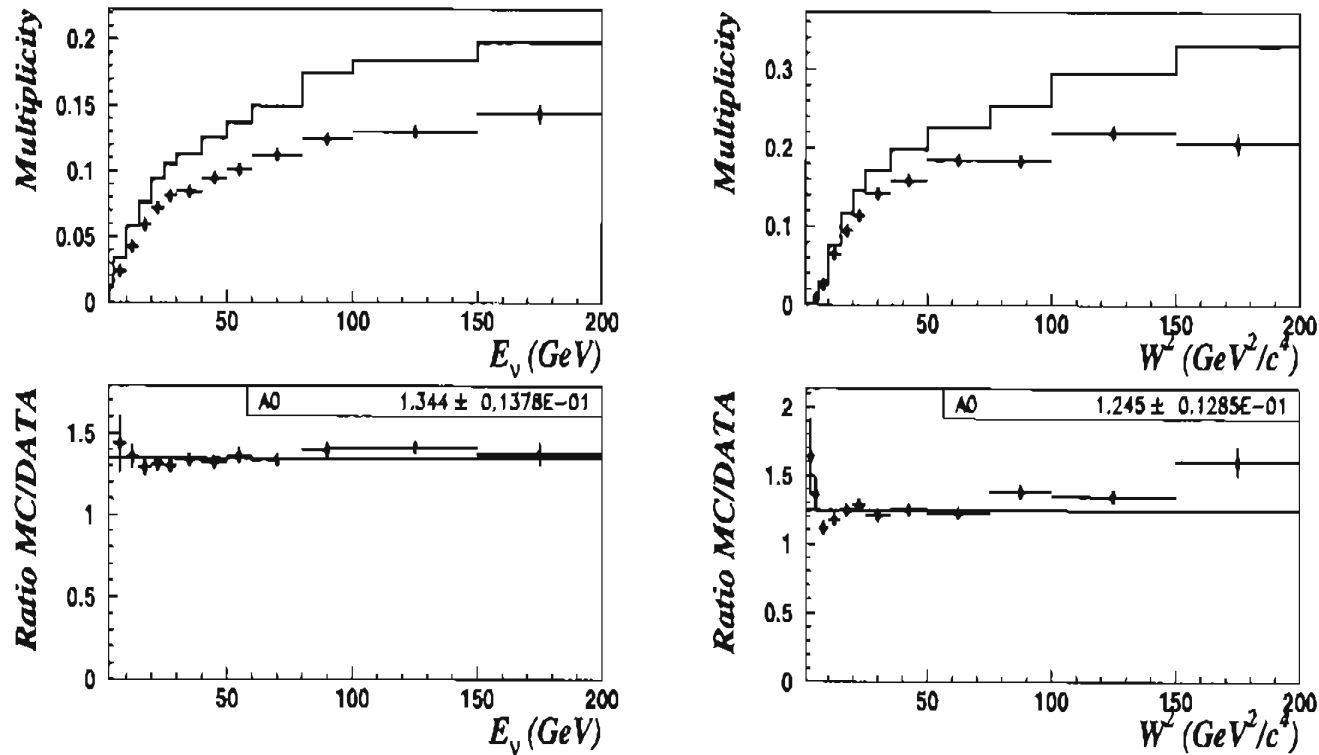


Figure 7: The multiplicity of K_S^0 and ratio MC/DATA as a function of E_ν and W_X , MC(histogram) calculation and the NOMAD data (points with errorbars).

(*P.Astier (NOMAD Coll.), Nucl.Phys.***B621**, (2002))

MC calculation of Λ^0 -spectra

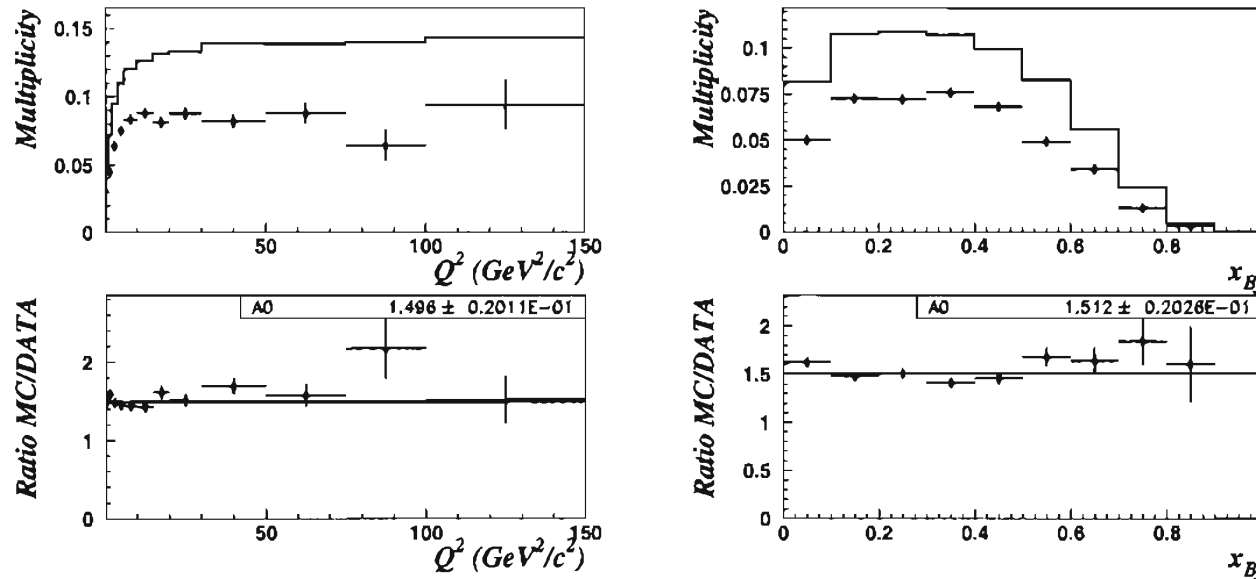


Fig. 7. Yields in the default MC (histogram) and in the data (points with error bars) for Λ as a function of E_ν , W^2 , Q^2 and x_{Bj} . The MC/Data ratios and their fit to a constant are also shown.

Figure 8: The multiplicity of Λ^0 and ratio MC/DATA as a function of Q^2 and x_B , MC(histogram) calculation and th NOMAD data (points with errorbars).

(*P.Astier (NOMAD Coll.), Nucl.Phys.***B621**, (2002))

MC calculation of Λ^0 -spectra

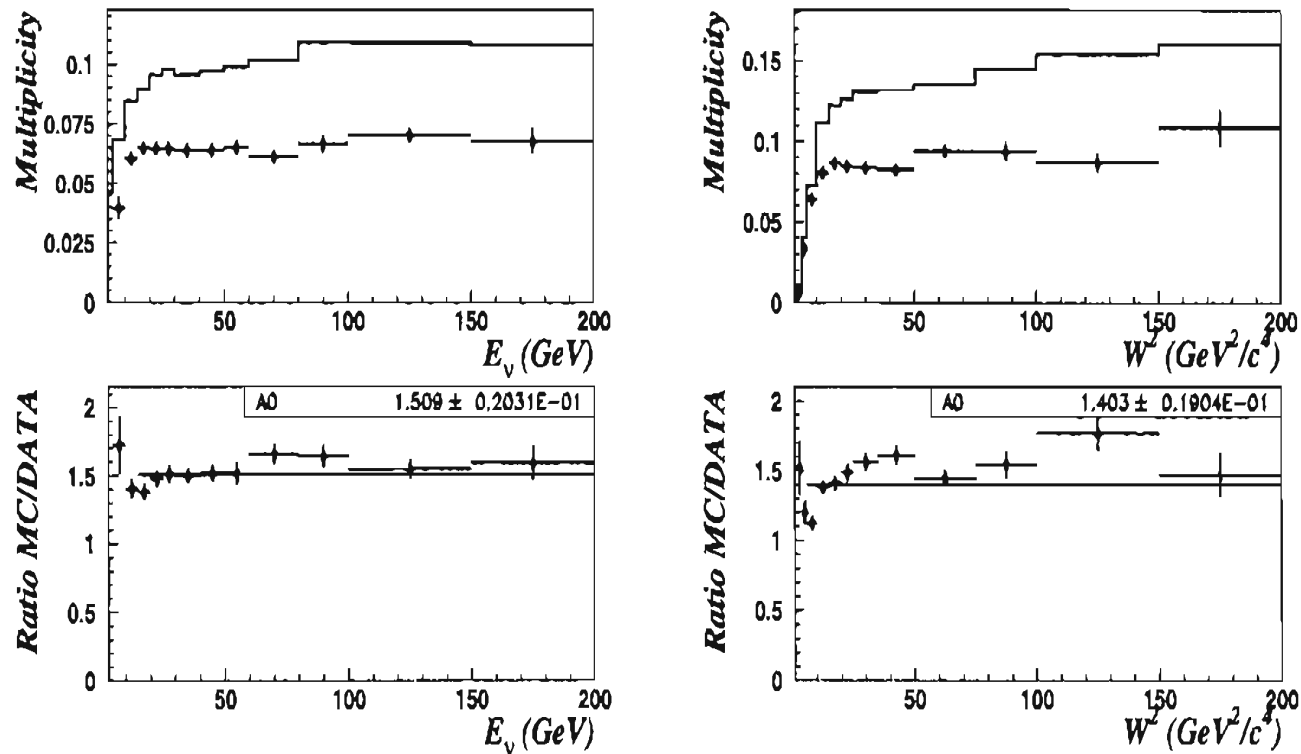


Figure 9: The multiplicity of Λ^0 and ratio MC/DATA as a function of E_ν and W_X , MC(histogram) calculation and the NOMAD data (points with errorbars).

(*P.Astier (NOMAD Coll.), Nucl.Phys.***B621**, (2002))

Theoretical framework

$$\rho_{lA \rightarrow l'hX} \equiv E_h \frac{d\sigma}{d^3p_h d\Omega dE'}(x, Q^2; z, p_t) ,$$

$$\rho_{lA \rightarrow l'hX}(x, Q^2; z, p_t) = \int_{z \leq y} dy d^2k_t f_A(y, Q^2, k_t) \times$$

$$\left[\frac{Z}{A} \rho_{lp \rightarrow l'hX}\left(\frac{x}{y}, Q^2; \frac{z}{y}, p_t - k_t\right) + \rho_{ln \rightarrow l'hX}\left(\frac{x}{y}, Q^2; \frac{z}{y}, p_t - k_t\right) \right] ,$$

where Z , N and A are the numbers of nucleons, protons and neutrons in the nucleus;

$$f_A(y, k_t) = \int dk_0 dk_z S(k) y \delta\left(y - \frac{M_A}{m} \frac{(kq)}{(P_A q)}\right)$$

Here $q^2 = -Q^2$, $S(k)$ is the relativistic invariant function describing the nuclear vertex with an outgoing virtual nucleon; $y = \frac{M_A}{m} \frac{(kp_\nu)}{(P_A q)}$

(*O. Benhar, S. Fantoni, G.L., N.V. Slavin, Phys.Rev.* **C57**, 1532 (1998))

Multiplicity of backward going charged pions

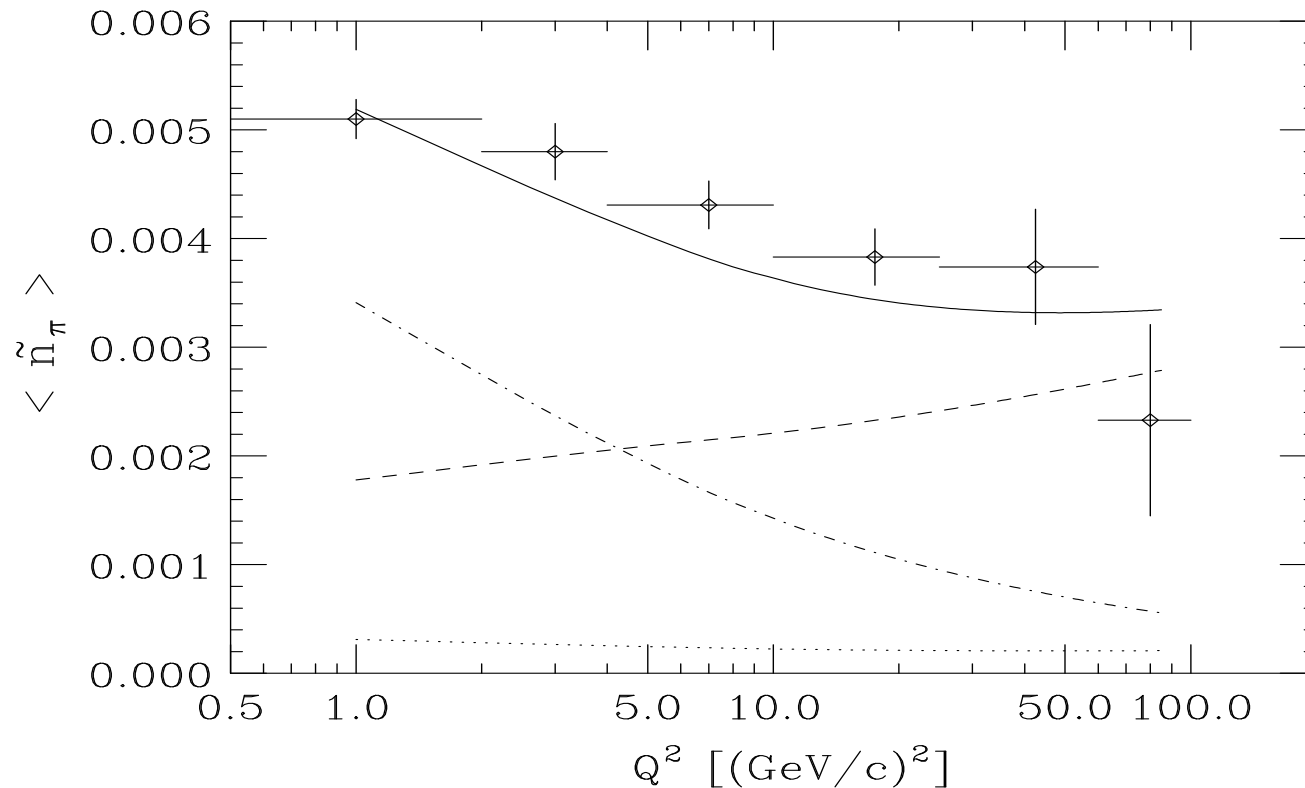


Figure 10: Mean multiplicity of charged pions produced in backward semi-sphere in $\nu^{12}C \rightarrow \mu^- \pi X$ process

(*P.Astier, et al., (NOMAD Coll.) Nucl.Phys..B609,255 (2001)*)

Our calculations

(*O.Benhar,S.Fantoni, G.L., U.Sukhatme, Phys.Lett.B527,73 (2002)*)

Backward going pions

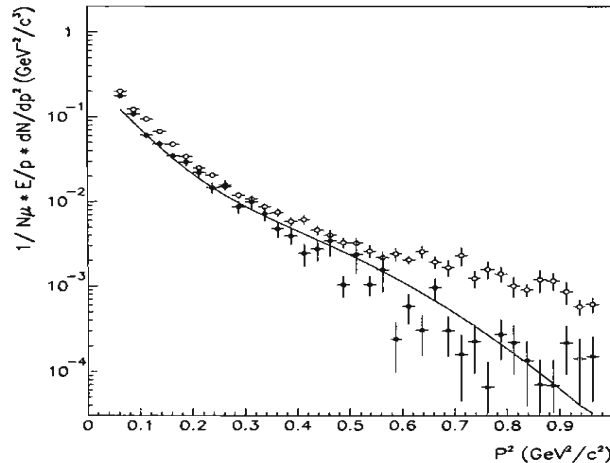


Fig. 13. Invariant spectrum for $B\pi^-$ in MC (open circles) and data (full circles). The solid line is the curve of Ref. [43] superimposed with an arbitrary normalization.

Figure 11: Comparison of our calculations (solid line) with the NOMAD data (full circles) and the MC calculation (open circles)

MC calculation and NOMAD data

(*P.Astier, et al., (NOMAD Coll.) Nucl.Phys..B609,255 (2001)*)

Our calculations

(*O.Benhar,S.Fantoni, G.L., Eur.Phys.J.A7,415 (2000);*

O.Benhar,S.Fantoni, G.L., U.Sukhatme, V.V.Uzhinsky,

Eur.Phys.J.A19,147 (2004))

SUMMARY

I. *The standard QCD model analyzing the multiple hadron production in lepton-proton interactions has to be corrected at $Q^2 < 10(\text{GeV}/c)^2$.*

II. *The non perturbative corrections can be included applying the $1/N$ expansion in QCD.*

III. *The inclusion of cylinder graphs or one-Pomeron exchange diagrams leads to satisfactory description of existing experimental data.*

IV. *Application of suggested approach and assuming an existence of non nucleon degrees of freedom in nuclei allows us to describe the NOMAD data on pion production in backward semi-sphere in $\nu - A$ semi-inclusive processes.*

V. *The suggested approach can be applied to analyze experiments like OPERA performed at the LNGS.*